A linear, mass conserved, energy stable scheme for Poisson-Nernst-Plank equations

Tian Qiao[a], Zhonghua Qiao[b], Shuyu Sun[a,*]

[a] *Computational Transport Phenomena Laboratory (CTPL), Physical Science and Engineering Division (PSE), King Abdullah University of Science and Technology (KAUST), Thuwal, 23955-6900, Saudi Arabia*

[b] *Department of Applied Mathematics, The Hong Kong Polytechnic University, Hung Hom, Kowloon, Hong Kong*

Abstract

In this paper, we introduce an efficient, stable, and accurate scheme for Poisson-Nernst-Plank (PNP) equations. The efficiency is improved from the previous non-linear scheme by linearized reformulation of the chemical potential. A novel technique, called energy factorization, is applied in the reformulation of PNP equations for the first time, so some desired properties at the discrete level are still preserved. They are unique solvability, mass conservation, and energy dissipation. It is proved that these properties are unconditionally preserved at the discrete level with our proposed scheme. We numerically demonstrate the accuracy of the scheme and simulate a two-species system. Analysis of the results verifies the expected numerical properties, and in particular, the positivity preservation of the concentration is testified numerically.

Keywords: Poisson-Nernst-Plank equations, mass conservation, energy stability, electric double layer

1. Introduction

Poisson-Nernst-Plank (PNP) equations are a set of partial differential equations which describe the transport of charged substances at the continuum level. The charged substance could be chemicals in the fluid medium and

*Corresponding author

Email address: shuyu.sun@kaust.edu.sa (Shuyu Sun)

ions through biological membranes, etc. Therefore, PNP equations serve as a popular model in various physical and biological applications [1; 2; 3; 4; 5]. Many efforts have been made to solve the equations analytically and numerically [6; 7; 8; 9; 10; 11; 12; 13]. However, the PNP equations naturally involve non-linear coupling between species concentration and electrical potential, so the analytical solutions are unavailable in most cases. As a result, the choice of an appropriate numerical scheme is essential for the solution to PNP equations.

A physical-meaningful result is one of the critical prerequisites for the numerical scheme. Concentration results are expected to satisfy certain conditions for the numerical results of PNP equations. For example, the total concentration should be conserved, and the concentration solution should always be positive. They are apparent in the physical model but not necessarily guaranteed for the numerical solution. In the last decades, many researchers have studied this area and proposed many schemes with different numerical methods like the finite difference method (FDM) and finite element method (FEM) [14; 15; 16; 17; 18]. Most of these schemes are proved to be mass conserved by the nature of the Nernst-Plank equation, but the positive concentration solution usually requires additional treatments. Recent literature reports various reformulation techniques (such as Slotboom transformation; logarithmic chemical potential) to achieve unconditional or conditional positivity [19; 20; 21; 22; 23; 24; 25; 26].

Stability, efficiency, and accuracy are also critical for the design of the numerical scheme. In recent decades, energy dissipation of numerical scheme has been applied as a critical criterion for different problems like Navier Stokes equations, equations of state, and phase-field model [27; 28; 29; 30; 31; 32; 33; 34; 35]. This is not only because dissipation of energy is expected from the physical perspective, but it also guarantees the numerical scheme's stability in a certain sense. Therefore, the energy dissipation of PNP equations at the discrete level has been demonstrated in many papers as well [36; 37; 38; 39]. Moreover, the balance between efficiency and accuracy is also extensively studied. Both efficient non-linear solver and direct linearized scheme are proposed to save computational time [40; 41; 42; 43; 44]. Nonetheless, we notice that the priority on efficiency often means the loss of other desired numerical properties. The energy factorization approach is proposed with this background [45]. It is initially for linearized reformulation of Peng-Robinson equation of state, while proved to satisfy energy stable condition.

In this paper, we propose a linear, mass conserved, energy stable scheme for the PNP equations. Unlike most of the classical schemes, the logarithm term in chemical potential is kept, although it results in additional nonlinearity. The energy factorization approach is applied to reformulate it, while the scheme after factorization can still satisfy desired numerical properties at the discrete level. The resulting semi-implicit time discrete scheme is therefore unique solvable, mass conserved, and energy stable. We apply CCFD for the spatial discretization and prove these properties are preserved in the fully discrete scheme. Validation of the scheme is conducted with a synthetical solution. Obtained results show that our scheme is first-order accurate in time and second-order accurate in space as expected. In addition to great accuracy, we also observe that the total concentration is conserved, and the total free energy is decaying during the simulation time. We specially testify the positivity of concentration results as well, and numerical experiments show the minimum concentration keeps positive even under extreme cases. Time evolution of concentration profiles is finally presented for multi-stage dynamics, and a classical 1D solution for EDL is recovered from it.

The rest of the paper is organized as follows. In section 2, we first introduce the formulation of PNP equations. In section 3, we propose the fully discrete scheme and prove that it enjoys three desired numerical properties. In section 4, numerical experiments are carried out to validate the proposed scheme. Finally, concluding remarks are provided in section 5.

2. Physical model

We consider a charged system within a bounded domain Ω. The dimensionless free energy F of the system is defined by

$$F = \int_\Omega \sum_{i=1}^{N} c_i(\log c_i - 1) + \frac{1}{2}(\rho_0 + \sum_{i=1}^{N} z_i c_i)\psi d\mathbf{x}, \tag{1}$$

where c_i is the dimensionless concentration of the i-th species in the system with N species of charged substances; ρ_0 is the dimensionless density of fixed charge; z_i is the valence of the i-th species.

The dimensionless PNP equations are then in the form of

$$\frac{\partial c_i}{\partial t} = \nabla \cdot (D_i c_i \nabla \mu_i), \tag{2}$$

$$\mu_i = \log c_i + z_i\psi, \tag{3}$$

$$-\nabla \cdot (\epsilon\ \nabla\psi) = \rho_0 + \sum_{i=1}^{N} z_i c_i, \tag{4}$$

where t is the dimenionless time; D_i is the diffusion constant of the i-th species; μ_i is the chemical potential w.r.t c_i; ϵ is the permittivity; ψ is the electrical potential.

We assume the boundary conditions for the system are periodic or homogeneous Neumann. These boundary conditions are necessary for total mass conservation, and they can greatly simplify the later derivation together with divergence theorem. Note here we first simplify the free energy and divide it into electrostatic and entropic contributions. They can be represented as

$$F^{electrostatic} = \frac{1}{2}\int_\Omega (\rho_0 + \sum_{i=1}^{N} z_i c_i)\psi d\mathbf{x}, \tag{5}$$

$$F^{entropic} = \int_\Omega \sum_{i=1}^{N} c_i(\log c_i - 1) d\mathbf{x}. \tag{6}$$

We substitute the equation (4) back into the formulation of electrostatic energy

$$F^{electrostatic} = \frac{1}{2}\int_\Omega (-\nabla \cdot (\epsilon\ \nabla\psi))\psi d\mathbf{x}. \tag{7}$$

With the Green's first identity and boundary condition, we have

$$\begin{aligned} F^{electrostatic} &= -\frac{1}{2}\int_\Omega \nabla \cdot (\psi^n \epsilon\ \nabla\psi^n) d\mathbf{x} + \frac{1}{2}\int_\Omega (\nabla\psi^n \cdot \epsilon\ \nabla\psi^n) d\mathbf{x} \\ &= \frac{1}{2}\int_\Omega \epsilon |\nabla\psi^n|^2 d\mathbf{x}. \end{aligned} \tag{8}$$

To solve the PNP equations (2-4), most literatures substitute the equation (3) back to equation (2) as

$$\frac{\partial c_i}{\partial t} = \nabla \cdot \left(D_i c_i \nabla(\log c_i + z_i\psi)\right), \tag{9}$$

and further simplify it with $c_i \nabla \log c_i = \nabla c_i$ to

$$\frac{\partial c_i}{\partial t} = \nabla \cdot \left(D_i(\nabla c_i + c_i \nabla z_i\psi)\right). \tag{10}$$

Different from most previous schemes, we keep the logarithm term and directly reformulate it as presented in the next section.

3. Numerical scheme

In this section, we apply cell-centered finite difference method for spatial discretization and present the fully discretized scheme. For simplicity, we only consider a rectangular computational domain Ω in 2D, but it is straightforward to extend it to the 3D case or reduce it to the 1D case. We cover $\Omega = [0, L_x] \times [0, L_y]$ with a uniform mesh size $h = x_{j+1} - x_j = y_{k+1} - y_k$, where $0 = x_0 \leq x_1 \leq \cdots \leq x_M = L_x$ and $0 = y_0 \leq y_1 \leq \cdots \leq y_W = L_y$. We evaluate all three euqations in the scheme at cell centers $(x_{j-\frac{1}{2}}, y_{k-\frac{1}{2}}) = (\frac{x_j - x_{j-1}}{2}, \frac{y_k - y_{k-1}}{2})$, $j = 1, 2, \cdots, M$ and $k = 1, 2, \cdots, W$.

To facilitate the derivation, we introduce the following discrete function spaces defined by

$$\nu_c = \{c : (x_{j-\frac{1}{2}}, y_{k-\frac{1}{2}}) \mapsto \mathbb{R},\ 1 \leq j \leq M,\ 1 \leq k \leq W\}, \tag{11}$$

$$\nu_u = \{u : (x_j, y_{k-\frac{1}{2}}) \mapsto \mathbb{R},\ 0 \leq j \leq M,\ 1 \leq k \leq W\}, \tag{12}$$

$$\nu_v = \{v : (x_{j-\frac{1}{2}}, y_k) \mapsto \mathbb{R},\ 1 \leq j \leq M,\ 0 \leq k \leq W\}. \tag{13}$$

For $c \in \nu_c$, we introduce the following discrete operators:

$$\delta_x^c[c]_{j,k-\frac{1}{2}} = \frac{c_{j+\frac{1}{2},k-\frac{1}{2}} - c_{j-\frac{1}{2},k-\frac{1}{2}}}{h}, \tag{14}$$

$$\delta_y^c[c]_{j-\frac{1}{2},k} = \frac{c_{j-\frac{1}{2},k+\frac{1}{2}} - c_{j-\frac{1}{2},k-\frac{1}{2}}}{h}, \tag{15}$$

$$A_x^c[c]_{j,k-\frac{1}{2}} = \frac{c_{j+\frac{1}{2},k-\frac{1}{2}} + c_{j-\frac{1}{2},k-\frac{1}{2}}}{2}, \tag{16}$$

$$A_y^c[c]_{j-\frac{1}{2},k} = \frac{c_{j-\frac{1}{2},k+\frac{1}{2}} + c_{j-\frac{1}{2},k-\frac{1}{2}}}{2}. \tag{17}$$

Apparently, $\delta_x^c[c]_{j,k-\frac{1}{2}},\ A_x^c[c]_{j,k-\frac{1}{2}} \in \nu_u$ and $\delta_y^c[c]_{j-\frac{1}{2},k},\ A_y^c[c]_{j-\frac{1}{2},k} \in \nu_v$. Similarly for $u \in \nu_u$ and $v \in \nu_v$, we define the following difference operators $\delta_x^u[u]_{j-\frac{1}{2},k-\frac{1}{2}},\ \delta_y^v[v]_{j-\frac{1}{2},k-\frac{1}{2}} \in \nu_c$:

$$\delta_x^u[u]_{j-\frac{1}{2},k-\frac{1}{2}} = \frac{u_{j,k-\frac{1}{2}} - u_{j-1,k-\frac{1}{2}}}{h}, \tag{18}$$

$$\delta_y^v[v]_{j-\frac{1}{2},k-\frac{1}{2}} = \frac{v_{j-\frac{1}{2},k} - v_{j-\frac{1}{2},k-1}}{h}. \tag{19}$$

With the defined discrete operator, we have the fully discrete scheme as

$$\frac{c_i^{n+1}-c_i^n}{\Delta t}=\delta_x^u[D_iA_x^c[c_i^n]\delta_x^c[\mu_i^{n+1}]]+\delta_y^v[D_iA_y^c[c_i^n]\delta_y^c[\mu_i^{n+1}]], \tag{20}$$

$$\mu_i^{n+1}=\log c_i^n+\frac{c_i^{n+1}}{c_i^n}-1+z_i\psi^{n+1}, \tag{21}$$

$$-\delta_x^u[\epsilon\delta_x^c[\psi^{n+1}]]-\delta_y^v[\epsilon\delta_y^c[\psi^{n+1}]]=\rho_0+\sum_{i=1}^{N}z_ic_i^{n+1}. \tag{22}$$

We then prove the following desired properties are preserved in this fully discrete scheme: (1) unique solvability, (2) mass conservation, (3) energy stability .

3.1. Unique solvability

Theorem 3.1. The proposed solution numerical scheme always possesses a unique solution $c^{n+1}\in\nu_c,\psi^{n+1}\in\nu_c$.

Proof. We define the following discrete inner products:

$$\langle c,\ C\rangle=h^2\sum_{j=1}^{M}\sum_{k=1}^{W}c_{j-\frac{1}{2},k-\frac{1}{2}}C_{j-\frac{1}{2},k-\frac{1}{2}},\ c,C\in\nu_c, \tag{23}$$

$$\langle u,\ U\rangle=h^2\sum_{j=1}^{M}\sum_{k=1}^{W}u_{j,k-\frac{1}{2}}U_{j,k-\frac{1}{2}},\ u,U\in\nu_u, \tag{24}$$

$$\langle v,\ V\rangle=h^2\sum_{j=1}^{M}\sum_{k=1}^{W}v_{j-\frac{1}{2},k}V_{j-\frac{1}{2},k},\ v,V\in\nu_v. \tag{25}$$

The discrete norms for $c\in\nu_c$,$u\in\nu_u$, and $v\in\nu_v$ are denoted by

$$||c||=\langle c,c\rangle^{1/2},||u||=\langle u,u\rangle^{1/2},||v||=\langle v,v\rangle^{1/2}. \tag{26}$$

We introduce two operators defined in papers [24; 26] to facilitate the derivation later, where

$$\mathcal{L}_hg=u,\ if\ g=-\nabla\cdot(\epsilon\nabla u), \tag{27}$$

$$\mathcal{L}_h^{'}g=u,\ if\ g=-\nabla\cdot(D_ic_i^n\nabla u). \tag{28}$$

By the definition of these operators, we have

$$\mathcal{L}_h(\rho_0 + \sum_{i=1}^{N} z_i c_i^{n+1}) = \psi^{n+1}, \tag{29}$$

$$\mathcal{L}_h^{'}(c_i^{n+1} - c_i^n) = -\Delta t \mu_i^{n+1}. \tag{30}$$

We can prove the numerical solution of the fully discrete scheme (equation (20 - 22)) is equivalent to the minimizer of a convex discrete functional:

$$\begin{aligned} I[c_i^{n+1}] = &\sum_{i=1}^{N} \langle c_i^{n+1}(\log c_i^n - 1) + \frac{(c_i^{n+1})^2}{2c_i^n} \ , \ 1\rangle \\ &+ \frac{1}{2\Delta t} \sum_{i=1}^{N} \langle c_i^{n+1} - c_i^n \ , \ \mathcal{L}_h^{'}(c_i^{n+1} - c_i^n)\rangle \\ &+ \frac{1}{2} \langle \mathcal{L}_h(\rho_0 + \sum_{i=1}^{N} z_i c_i^{n+1}) \ , \ \rho_0 + \sum_{i=1}^{N} z_i c_i^{n+1}\rangle. \end{aligned} \tag{31}$$

Therefore, the solution must be unique, and the unique solvability is proved.

3.2. Mass conservation

Theorem 3.2. The total concentration for all species is constant with time.

$$\sum_{j=1}^{M}\sum_{k=1}^{W} (c_i^{n+1})_{j-\frac{1}{2},k-\frac{1}{2}} = \sum_{j=1}^{M}\sum_{k=1}^{W} (c_i^n)_{j-\frac{1}{2},k-\frac{1}{2}}. \tag{32}$$

Proof. Summing both sides of Equation (20) over j, k, we have

$$\begin{aligned} \sum_{j=1}^{M}\sum_{k=1}^{W} \frac{(c_i^{n+1})_{j-\frac{1}{2},k-\frac{1}{2}} - (c_i^n)_{j-\frac{1}{2},k-\frac{1}{2}}}{\Delta t} = &\sum_{j=1}^{M}\sum_{k=1}^{W} (\delta_x^u[D_i A_x^c[c_i^n]\delta_x^c[\mu_i^{n+1}]])_{j-\frac{1}{2},k-\frac{1}{2}} \\ &+ \sum_{j=1}^{M}\sum_{k=1}^{W} (\delta_y^v[D_i A_y^c[c_i^n]\delta_y^c[\mu_i^{n+1}]])_{j-\frac{1}{2},k-\frac{1}{2}}. \end{aligned} \tag{33}$$

By the boundary conditions, the right-hand side becomes zero with the summation by parts. We read the left-hand side, and this gives us the mass conservation.

$$\sum_{j=1}^{M}\sum_{k=1}^{W}(c_i^{n+1})_{j-\frac{1}{2},k-\frac{1}{2}} = \sum_{j=1}^{M}\sum_{k=1}^{W}(c_i^{n})_{j-\frac{1}{2},k-\frac{1}{2}}. \tag{34}$$

3.3. Energy stability

Theorem 3.3. The total energy of the system keeps dissipated over time, where the discrete total free energy is defined as

$$F_h^n = \sum_{i=1}^{N}\langle c_i^n,\ \log c_i^n - 1\rangle + \frac{1}{2}\langle \rho_0 + \sum_{i=1}^{N} z_i c_i^n, \psi^n\rangle. \tag{35}$$

Proof. We substitute the equation 22 into the energy functional

$$F_h^n = \sum_{i=1}^{N}\langle c_i^n,\ \log c_i^n - 1\rangle + \frac{1}{2}\langle -\delta_x^u[\epsilon\delta_x^c[\psi^n]] - \delta_y^v[\epsilon\delta_y^c[\psi^n]], \psi^n\rangle. \tag{36}$$

With the boundary conditions on summation by parts, we have

$$\begin{aligned} F_h^n &= \sum_{i=1}^{N}\langle c_i^n,\ \log c_i^n - 1\rangle + \frac{1}{2}\epsilon\langle \delta_x^c[\psi^n], \delta_x^c[\psi^n]\rangle + \frac{1}{2}\epsilon\langle \delta_y^c[\psi^n], \delta_y^c[\psi^n]\rangle \\ &= \sum_{i=1}^{N}\langle c_i^n,\ \log c_i^n - 1\rangle + \frac{1}{2}\epsilon(||\delta_x^c[\psi^n]||^2 + ||\delta_y^c[\psi^n]||^2). \end{aligned} \tag{37}$$

We shall examine the energy difference between two neighboring time steps as

$$\begin{aligned} F_h^{n+1} - F_h^n &= \sum_{i=1}^{N}(\langle c_i^{n+1},\ \log c_i^{n+1} - 1\rangle - \langle c_i^n,\ \log c_i^n - 1\rangle) \\ &+\frac{1}{2}\epsilon(||\delta_x^c[\psi^{n+1}]||^2 + ||\delta_y^c[\psi^{n+1}]||^2 - ||\delta_x^c[\psi^n]||^2 - ||\delta_y^c[\psi^n]||^2). \end{aligned} \tag{38}$$

Note we treat the chemical potential in a semi-implicit manner in our proposed scheme. This formulation is actually derived from the energy factorization approach [45] to resolve the non-linearity. It raises from the concavity of the logarithm function. For any two neighboring time steps $n+1$

and n, we have

$$\langle \log c_i^{n+1} - \log c_i^n, 1 \rangle \leq \langle \frac{1}{c_i^n}, c_i^{n+1} - c_i^n \rangle. \tag{39}$$

Equation (39) can greatly simplify the derivation for energy dissipation in a way that

$$\begin{aligned} &\sum_{i=1}^{N} (\langle c_i^{n+1},\ \log c_i^{n+1} - 1 \rangle - \langle c_i^n,\ \log c_i^n - 1 \rangle) \\ &\leq \sum_{i=1}^{N} \langle \log c_i^n + \frac{c_i^{n+1}}{c_i^n} - 1, c_i^{n+1} - c_i^n \rangle, \end{aligned} \tag{40}$$

The following inequality can also be readily proved:

$$\begin{aligned} &\frac{1}{2}\epsilon(||\delta_x^c[\psi^{n+1}]||^2 + ||\delta_y^c[\psi^{n+1}]||^2 - ||\delta_x^c[\psi^n]||^2 - ||\delta_y^c[\psi^n]||^2) \\ &\leq \sum_{i=1}^{N} \langle\ z_i \psi^{n+1}\ , c_i^{n+1} - c_i^n \rangle. \end{aligned} \tag{41}$$

Combining inequalities in equation (40) and equation (41), we have

$$\begin{aligned} F_h^{n+1} - F_h^n &\leq \sum_{i=1}^{N} \langle\ \log c_i^n + \frac{c_i^{n+1}}{c_i^n} - 1 + z_i \psi^{n+1}\ , c_i^{n+1} - c_i^n \rangle \\ &= \sum_{i=1}^{N} \langle\ \mu_i^{n+1}\ , c_i^{n+1} - c_i^n \rangle. \end{aligned} \tag{42}$$

We then substitute equation (20) from our proposed scheme to reach the energy dissipation.

$$\begin{aligned} F_h^{n+1} - F_h^n &\leq -\sum_{i=1}^{N} \Delta t D_i (A_x^c[c_i^n] \langle \delta_x^c[\mu_i^{n+1}], \delta_x^c[\mu_i^{n+1}] \rangle + A_y^c[c_i^n] \langle \delta_y^c[\mu_i^{n+1}], \delta_y^c[\mu_i^{n+1}] \rangle) \\ &= -\sum_{i=1}^{N} \Delta t D_i (A_x^c[c_i^n]\ ||\delta_x^c[\mu_i^{n+1}]||^2 + A_y^c[c_i^n]\ ||\delta_y^c[\mu_i^{n+1}]||^2) \leq 0. \end{aligned} \tag{43}$$

It is clear that

$$F_h^{n+1} \leq F_h^n, \tag{44}$$

and we complete the proof of energy dissipation.

4. Numerical Experiments

In this section, we present the results obtained from our proposed numerical scheme (equation (20 - 22)). Order of convergence is first testified with a synthetic exact solution. Three case studies are then conducted for sodium-chloride saline solution. Obtained results are analysed to show that the properties we prove analytically in the previous section is indeed preserved in numerical simulation. Positivity preserving of concentration solution is also numerically testified among them.

4.1. Convergence test

We first perform the numerical experiments for convergence test. For simplicity, an exact solution with only two species is first constructed as

$$c_1(x, y, t) = (1 - \exp(-t)) \sin(\pi x) \cos(\pi y) + 2, \tag{45}$$

$$c_2(x, y, t) = (1 - \exp(-t)) \sin(\pi x) \cos(\pi y) + 2, \tag{46}$$

$$\psi(x, y, t) = -\exp(-t) \cos(\pi x) \sin(\pi y). \tag{47}$$

To recover the exact solution with our proposed scheme, we choose the computational domain $\Omega = [0, 2] \times [0, 2]$, so the periodic boundary condition should naturally hold by the definition of trigonometric functions for exact solutions. Initial conditions and fixed charge distribution for numerical simulation can be computed from the exact solution as the input. We set other constant parameters $D_1, D_2, \epsilon = 1$ in this case, and valence $z_1 = 1, z_2 = -1$ are assigned to the two species.

We then conduct the numerical convergence study with different mesh sizes and time steps. Both L^2 and L^∞ discrete norm are computed for the difference of c_1 between the obtained numerical results and exact solutions. From the results reported in table 1 and table 2, we can conclude that our scheme is indeed first-order accurate in time and second-order accurate in space as expected.

h	Δt	L^2 error	order	L^∞ error	order
0.2	0.2	0.42648	-	0.49817	-
0.1	0.1	0.15304	1.4786	0.20566	1.2764
0.05	0.05	0.066913	1.1935	0.09204	1.1599
0.025	0.025	0.031683	1.0786	0.043328	1.0870
0.0125	0.0125	0.015474	1.0339	0.020989	1.0456

Table 1: L^2 and L^∞ error and convergence order for c_1 with $\Delta t = h$.

h	Δt	L^2 error	order	L^∞ error	order
0.2	0.04	0.029158	-	0.039394	-
0.1	0.01	0.0089917	1.6972	0.013485	1.5466
0.05	0.0025	0.0023119	1.9595	0.003597	1.9065
0.025	0.000625	0.00057635	2.0040	0.000922	1.9640
0.0125	0.00015625	0.00014332	2.0077	0.00023318	1.9833

Table 2: L^2 and L^∞ error and convergence order for c_1 with $\Delta t = h^2$.

4.2. Simulations of sodium-chloride saline solution.

We next perform our numerical experiments in 2D to simulate a sodium-chloride saline solution. The computational domain is $\Omega = [0, 6] \times [0, 6]$, and mesh size now is 0.05. For the initial condition, we randomly sample the concentration for two species with mean concentration of 0.5 on the entire domain. Positive fixed charges with $\rho_0 = 1.5$ are placed at $x = 1.5$, and negative charges with $\rho_0 = -1.5$ are placed symmetrically at $x = 4.5$. We set constant parameters $D_1, D_2 = 0.304, \epsilon = 0.185, z_1 = 1, z_2 = -1$ respectively. We then run the simulation for 300 steps with the time step $\Delta t = 0.01$ until the steady state. Concentration profile for the anion are plotted in Fig.1.

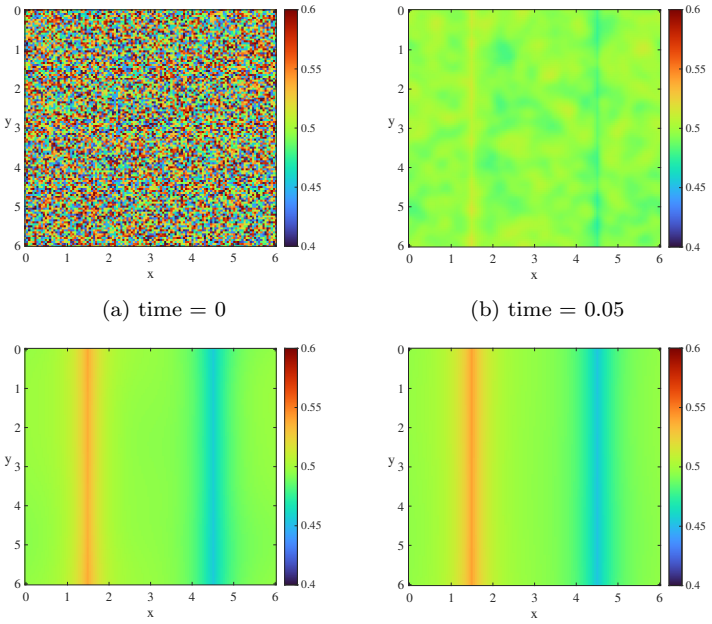

(a) time = 0 (b) time = 0.05

(c) time = 1 (d) time = 3

Figure 1: Concentration profile at different time.

Two stages of dynamics can be observed from the results. Starting from the heterogeneous initial condition, the ions distribution turns homogeneous rapidly at $t = 0.05$ due to diffusion. After that, the electrical force dominates the second stage. Two fixed charge stripes attract opposite ions while repulsing the others, and reach the steady-state at $t = 3$. This case follows a study recently reported in literature [24] for a nonlinear PNP scheme, in which the logarithm term is also kept for energy stability but results in additional nonlinearity. Our results show a fairly similar evolution to the previous scheme. Our scheme, however, is anticipated to be more effective because each time step only requires the solution of a linear system. Fig. 2 shows the evaluation of expected properties from obtained results. The constant total concentration result numerically proves the mass conservation, as the total free energy keeps dissipating during the simulation time.

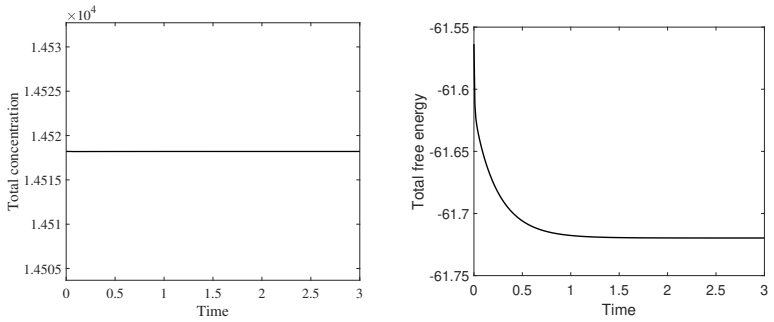

(a) total concentration of all species (b) total free energy of the system

Figure 2: Evaluation of physics properties from numerical results.

We then push the numerical cases to the extreme by increasing the fixed charge density to $\rho_0 = 100$ and $\rho_0 = -100$ respectively. A large blank area can be observed in the steady-state results from Fig.3a. This is because most of the ions are attracted to $x = 1.5$ due to strong attraction while acting to heavy repulsion at $x = 4.5$. Under this extreme scenario, the concentration solutions at most of the location are close to zero. Nevertheless, our scheme can still ensure the positivity of the numerical solution, because the minimum concentration is always great than zero (Fig.3b).

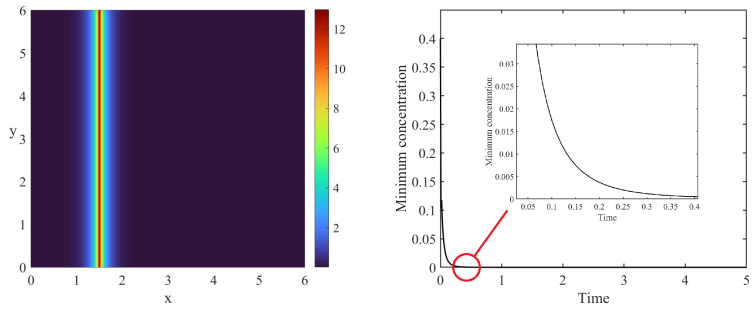

(a) concentration at $t = 3$ (b) minimum concentration

Figure 3: Numerical results from the 2D extreme case.

We next reset the location of fixed charge stripes to simulate the classical electrical double layer case [7; 10; 14]. They are now distributed at $x = 0$ and $x = 6$ to simulate the ions that are absorbed into the walls of a parallel channel. We modify the fixed charge density for two stripes to be $\rho_0 = 1.5$ so the solution is symmetrical across the x-direction. The initial condition

is also reset to be the homogeneous distribution for two ions respectively to satisfy the neutrality compatible condition. Fig.4 shows the results for both electrical potential and ion concentration. Symmetrical 2D results are reduced to 1D with given y-coordinates and half length in the x-direction. Time evolution profile is provided from initial state to steady state for the concentration of both ions. They are agreeing with the results we would anticipate from 1D solutions.

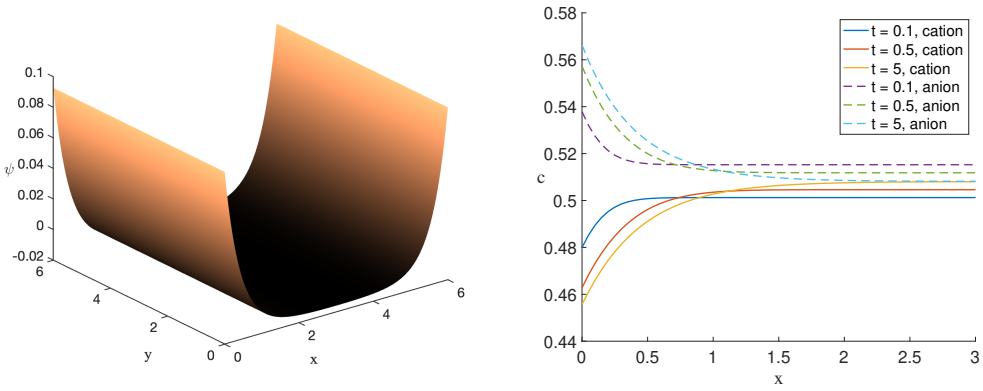

(a) 2D electrical potential distribution

(b) species concentration at $y = 3$

Figure 4: Results for 2D with the existence of EDL.

5. Conclusion

A linear numerical scheme is proposed for PNP equations in this paper. The energy factorization approach is applied to formulate this scheme and preserve desired numerical properties at the discrete level. We prove that unique solvability, mass conservation, and energy dissipation are unconditionally kept with the fully discrete schemes. These properties are further validated with numerical experiments. Moreover, positivity preserving for concentration solution is also numerically testified. We expect this scheme to be implemented in more computational applications as its high efficiency and other superior properties.

Acknowledgements

We would like to thank for the research funding from King Abdullah University of Science and Technology (KAUST) through the grants BAS/1/1351-01, URF/1/4074-01, and URF/1/3769-01.

Competing interests statement

The authors declare that they have no known competing financial interests or personal relationships that could have appeared to influence the work reported in this paper.

References

[1] M. Z. Bazant, K. Thornton, A. Ajdari, Diffuse-charge dynamics in electrochemical systems, Physical Review E - Statistical Physics, Plasmas, Fluids, and Related Interdisciplinary Topics 70 (2) (2004) 24.

[2] T. R. Brumleve, R. P. Buck, Numerical solution of the Nernst-Planck and poisson equation system with applications to membrane electrochemistry and solid state physics, Journal of Electroanalytical Chemistry and Interfacial Electrochemistry 90 (1) (1978) 1–31.

[3] T. L. Horng, T. C. Lin, C. Liu, B. Eisenberg, PNP Equations with Steric Effects: A Model of Ion Flow through Channels, Journal of Physical Chemistry B 116 (37) (2012) 11422–11441.

[4] Y. Yang, R. A. Patel, S. V. Churakov, N. I. Prasianakis, G. Kosakowski, M. Wang, Multiscale modeling of ion diffusion in cement paste: electrical double layer effects, Cement and Concrete Composites 96 (2019) 55–65.

[5] Q. Zheng, D. Chen, G. W. Wei, Second-order Poisson–Nernst–Planck solver for ion transport, Journal of Computational Physics 230 (13) (2011) 5239–5262.

[6] M. S. Kilic, M. Z. Bazant, A. Ajdari, Steric effects in the dynamics of electrolytes at large applied voltages. I. Double-layer charging, Physical Review E - Statistical, Nonlinear, and Soft Matter Physics 75 (2) (2007) 021502.

[7] M. S. Kilic, M. Z. Bazant, A. Ajdari, Steric effects in the dynamics of electrolytes at large applied voltages. II. Modified Poisson-Nernst-Planck equations, Physical Review E - Statistical, Nonlinear, and Soft Matter Physics 75 (2) (2007) 021503.

[8] C. C. Lee, H. Lee, Y. K. Hyon, T. C. Lin, C. Liu, New Poisson–Boltzmann type equations: one-dimensional solutions, Nonlinearity 24 (2) (2010) 431.

[9] T. C. Lin, B. Eisenberg, Multiple solutions of steady-state Poisson–Nernst–Planck equations with steric effects, Nonlinearity 28 (7) (2015) 2053.

[10] R. Morrow, D. R. McKenzie, M. M. Bilek, The time-dependent development of electric double-layers in saline solutions, Journal of Physics D: Applied Physics 39 (5) (2006) 937–943.

[11] M. Wang, S. Chen, Electroosmosis in homogeneously charged micro- and nanoscale random porous media, Journal of Colloid and Interface Science 314 (1) (2007) 264–273.

[12] V. R. Hsu, Almost Newton method for large flux steady-state of 1D Poisson–Nernst–Planck equations, Journal of Computational and Applied Mathematics 183 (1) (2005) 1–15.

[13] R. Aitbayev, P. W. Bates, H. Lu, L. Zhang, M. Zhang, Mathematical studies of Poisson–Nernst–Planck model for membrane channels: Finite ion size effects without electroneutrality boundary conditions, Journal of Computational and Applied Mathematics 362 (2019) 510–527.

[14] A. Flavell, M. Machen, B. Eisenberg, J. Kabre, C. Liu, X. Li, A. Flavell, ·. M. Machen, ·. J. Kabre, ·. X. Li, M. Machen, B. Eisenberg, C. Liu, A conservative finite difference scheme for Poisson-Nernst-Planck equations, J Comput Electron 13 (2014) 235–249.

[15] H. Liu, Z. Wang, A free energy satisfying discontinuous Galerkin method for one-dimensional Poisson–Nernst–Planck systems, Journal of Computational Physics 328 (2017) 413–437.

[16] J. Ding, Z. Wang, S. Zhou, Positivity preserving finite difference methods for Poisson–Nernst–Planck equations with steric interactions: Application to slit-shaped nanopore conductance, Journal of Computational Physics 397 (2019) 108864.

[17] C. Liu, C. Wang, S. M. Wise, X. Yue, S. Zhou, An iteration solver for the Poisson–Nernst–Planck system and its convergence analysis, Journal of Computational and Applied Mathematics 406 (2022) 114017.

[18] G. Ji, W. Zhu, A weak Galerkin finite element method for time-dependent Poisson–Nernst–Planck equations, Journal of Computational and Applied Mathematics 416 (2022) 114563.

[19] D. He, K. Pan, X. Yue, A Positivity Preserving and Free Energy Dissipative Difference Scheme for the Poisson–Nernst–Planck System, Journal of Scientific Computing 81 (1) (2019) 436–458.

[20] J. Hu, X. Huang, A fully discrete positivity-preserving and energy-dissipative finite difference scheme for Poisson–Nernst–Planck equations, Numerische Mathematik 145 (1) (2020) 77–115.

[21] F. Huang, J. Shen, Bound/positivity preserving and energy stable scalar auxiliary variable schemes for dissipative systems: Applications to Keller-Segel and Poisson-Nernst-Planck equations, SIAM Journal on Scientific Computing 43 (3) (2021) A1832–A1857.

[22] H. Liu, W. Maimaitiyiming, Efficient, Positive, and Energy Stable Schemes for Multi-D Poisson–Nernst–Planck Systems, Journal of Scientific Computing 87 (3) (2021) 1–36.

[23] H. Liu, Z. Wang, A free energy satisfying finite difference method for Poisson–Nernst–Planck equations, Journal of Computational Physics 268 (2014) 363–376.

[24] Y. Qian, C. Wang, S. Zhou, A positive and energy stable numerical scheme for the Poisson–Nernst–Planck–Cahn–Hilliard equations with steric interactions, Journal of Computational Physics 426 (2021) 109908.

[25] Z. Qiao, Z. Xu, Q. Yin, S. Zhou, Structure-preserving numerical method for Ampere-Nernst-Planck model (2022). arXiv:2204.11743.

[26] J. Shen, J. Xu, Unconditionally positivity preserving and energy dissipative schemes for Poisson–Nernst–Planck equations, Numerische Mathematik 148 (3) (2021) 671–697.

[27] H. Chen, S. Sun, T. Zhang, Energy Stability Analysis of Some Fully Discrete Numerical Schemes for Incompressible Navier–Stokes Equations on Staggered Grids, Journal of Scientific Computing 75 (1) (2018) 427–456.

[28] H. Chen, S. Sun, T. Zhang, Energy Stability Analysis of Some Fully Discrete Numerical Schemes for Incompressible Navier–Stokes Equations on Staggered Grids, Journal of Scientific Computing 75 (1) (2018) 427–456.

[29] X. Feng, J. Kou, S. Sun, A Novel Energy Stable Numerical Scheme for Navier-Stokes-Cahn-Hilliard Two-Phase Flow Model with Variable Densities and Viscosities, Computational Science – ICCS 2018. ICCS 2018. Lecture Notes in Computer Science 10862 LNCS (2018) 113–128.

[30] X. Feng, M. H. Chen, Y. Wu, S. Sun, A fully explicit and unconditionally energy-stable scheme for Peng-Robinson VT flash calculation based on dynamic modeling, Journal of Computational Physics 463 (2022) 111275.

[31] J. Kou, S. Sun, X. Wang, Linearly Decoupled Energy-Stable Numerical Methods for Multicomponent Two-Phase Compressible Flow, SIAM Journal on Numerical Analysis 56 (6) (2018) 3219–3248.

[32] J. Kou, X. Wang, S. Du, S. Sun, An energy stable linear numerical method for thermodynamically consistent modeling of two-phase incompressible flow in porous media, Journal of Computational Physics 451 (2022) 110854.

[33] G. Zhu, H. Chen, J. Yao, S. Sun, Efficient energy-stable schemes for the hydrodynamics coupled phase-field model, Applied Mathematical Modelling 70 (2019) 82–108.

[34] G. Zhu, H. Chen, A. Li, S. Sun, J. Yao, Fully discrete energy stable scheme for a phase-field moving contact line model with variable densities and viscosities, Applied Mathematical Modelling 83 (2020) 614–639.

[35] X. Li, Z. H. Qiao, H. Zhang, An unconditionally energy stable finite difference scheme for a stochastic Cahn-Hilliard equation, Science China Mathematics 2016 59:9 59 (9) (2016) 1815–1834.

[36] A. Flavell, J. Kabre, X. Li, An energy-preserving discretization for the Poisson–Nernst–Planck equations, Journal of Computational Electronics 16 (2) (2017) 431–441.

[37] Z. Qiao, Z. Xu, Q. Yin, S. Zhou, An Ampére-Nernst-Planck Framework for Modeling Charge Dynamics (2022). arXiv:2202.07366.

[38] H. Liu, Z. Wang, A free energy satisfying discontinuous Galerkin method for one-dimensional Poisson–Nernst–Planck systems, Journal of Computational Physics 328 (2017) 413–437.

[39] C. Liu, C. Wang, S. M. Wise, X. Yue, S. Zhou, A positivity-preserving, energy stable and convergent numerical scheme for the Poisson-Nernst-Planck system, Mathematics of Computation 90 (331) (2021) 2071–2106.

[40] C. Liu, C. Wang, S. M. Wise, X. Yue, S. Zhou, An iteration solver for the Poisson–Nernst–Planck system and its convergence analysis, Journal of Computational and Applied Mathematics 406 (2022) 114017.

[41] J. Ding, Z. Wang, S. Zhou, Structure-preserving and efficient numerical methods for ion transport, Journal of Computational Physics 418 (2020) 109597.

[42] H. Gao, D. He, Linearized Conservative Finite Element Methods for the Nernst–Planck–Poisson Equations, Journal of Scientific Computing 72 (3) (2017) 1269–1289.

[43] H. Gao, P. Sun, A Linearized Local Conservative Mixed Finite Element Method for Poisson–Nernst–Planck Equations, Journal of Scientific Computing 77 (2) (2018) 793–817.

[44] D. He, K. Pan, An energy preserving finite difference scheme for the Poisson–Nernst–Planck system, Applied Mathematics and Computation 287-288 (2016) 214–223.

[45] J. Kou, S. Sun, X. Wang, A novel energy factorization approach for the diffuse-interface model with peng-robinson equation of state, SIAM Journal on Scientific Computing 42 (1) (2020) B30–B56.